

## Dipolar relaxation collisions in magnetically trapped ${}^7\text{Li}$

J. M. Gerton, C. A. Sackett, B. J. Frew, and R. G. Hulet

*Department of Physics and Rice Quantum Institute, Rice University, Houston, Texas 77251*

(Received 22 September 1998)

We report the measurement of the rate constant for dipolar relaxation from the ( $F=2$ ,  $m_F=2$ ) hyperfine state of  ${}^7\text{Li}$ . The atoms are confined in a permanent magnet trap at a field of  $10^3$  G. The measured value of  $(1.05 \pm 0.10) \times 10^{-14}$   $\text{cm}^3/\text{s}$  agrees well with theory. Additionally, we determine an upper bound for the three-body molecular recombination rate constant of  $10^{-27}$   $\text{cm}^6/\text{s}$ , which is also consistent with predictions. [S1050-2947(99)05502-X]

PACS number(s): 03.75.Fi, 32.80.Pj, 34.50.-s

Ultracold atom collisions are important in many studies of trapped atomic gases. For example, collisions between ground-state atoms play a critical role in the evaporative cooling process which was used to achieve Bose-Einstein condensation (BEC) of magnetically trapped, dilute atomic gases [1–3]. During evaporation, elastic collisions drive the gas towards thermal equilibrium while inelastic collisions lead to loss of atoms from the trap. Thus, the ratio of elastic to inelastic collision rates determines the efficiency of evaporative cooling. Knowledge of these rates facilitates the optimization of cooling so that the maximum increase in phase-space density is obtained [4,5]. Collisions also critically influence the dynamical behavior of ultracold gases and of BEC in particular. Condensate formation rates, decay rates, coherence times, and many other dynamical properties are governed by collisional interactions. Accurate measurements of inelastic collision rate constants provide important feedback for theoretical models of these processes.

Inelastic collision rate constants can be determined from the rate that atoms are lost from a trap. The four predominant collisional loss mechanisms for magnetically trapped atoms are (i) collisions with background gas, (ii) magnetic dipolar relaxation, (iii) spin exchange, and (iv) three-body recombination. For the  ${}^7\text{Li}$  BEC experiments described in Refs. [2,6,7], the atoms are confined in the doubly spin-polarized ( $F=2$ ,  $m_F=2$ ) hyperfine state from which spin exchange is impossible. Dipolar relaxation is the dominant loss mechanism at the very low background-gas pressures and relatively low trapped-atom densities of these experiments. In this paper, we report the dipolar relaxation rate constant obtained from trap-loss measurements of a nondegenerate gas of  ${}^7\text{Li}$ .

The theory for dipolar relaxation collisions at low temperatures was initially developed for spin-polarized hydrogen [8,9]. The predicted rate constants for hydrogen are consistent with experimental measurements [10–12] and are of order  $10^{-15}$   $\text{cm}^3/\text{s}$ . However, the situation is less clear for the alkali-metal elements. Recently, the measured value of the dipolar relaxation rate constant for the doubly spin-polarized state of cesium was shown to depend strongly on temperature due to the presence of a zero-energy resonance [13]. The value was measured to be  $4 \times 10^{-12}$   $\text{cm}^3/\text{s}$  at 8  $\mu\text{K}$ , nearly three orders of magnitude larger than predicted [14]. Also, measurements of the spin relaxation rate of near-room-temperature, spin-polarized rubidium vapor have revealed a magnetic field dependence which is not yet understood [15].

Dipolar relaxation collisions arise from the magnetic dipole-dipole interaction between the magnetic moments of two colliding atoms [8]. The spatial and spin parts of the two-body wave function are coupled by the interaction Hamiltonian  $H_{\text{dip}} \propto \mathbf{F}_1 \cdot \mathbf{F}_2 / R^3$ , where  $\mathbf{F}_i$  is the total spin angular momentum of atom  $i$  and  $R$  is the interatomic distance. One or both of the  ${}^7\text{Li}$  atoms initially in the doubly spin-polarized ( $F=2$ ,  $m_F=2$ ) state can emerge from the collision in a different spin state. The Zeeman or hyperfine energy released is shared equally between the atoms since they are nearly at rest initially. These collisions result in trap loss if either of the atoms emerges in an untrapped high-field-seeking spin state, or if the kinetic energy gained by the pair is larger than the trap potential depth.

The trap loss rate of a freely evolving gas is

$$\dot{N} = - \int d^3r \Gamma(\mathbf{r}) n(\mathbf{r}), \quad (1)$$

where  $N$  is the total number of trapped atoms,  $n(\mathbf{r})$  is the atom density at position  $\mathbf{r}$ , and  $\Gamma(\mathbf{r})$  is the position-dependent loss rate. For the present experiment, the trap potential depth is much less than the energy liberated by dipolar relaxation or three-body recombination. Therefore, all atoms participating in such collisions are ejected and  $\Gamma$  is given by

$$\Gamma(\mathbf{r}) = G_1 + 2G_2 n(\mathbf{r}) + 3G_3 n^2(\mathbf{r}), \quad (2)$$

where  $G_1$ ,  $G_2$ , and  $G_3$  are the rate constants for background-gas collisional loss, dipolar relaxation, and three-body recombination, respectively. For a nondegenerate gas in thermal equilibrium at temperature  $T$ , the density is given by

$$n(\mathbf{r}) = N \left( \frac{m \bar{\omega}^2}{2\pi k_B T} \right)^{3/2} e^{-u(\mathbf{r})/k_B T}, \quad (3)$$

where  $m$  is the atomic mass,  $u(\mathbf{r}) = \frac{1}{2} m (\omega_x^2 x^2 + \omega_y^2 y^2 + \omega_z^2 z^2)$  is the harmonic confining potential, and  $\bar{\omega} = (\omega_x \omega_y \omega_z)^{1/3}$ . Assuming this density distribution, Eq. (1) can be integrated to give the loss rate per trapped atom,

$$\frac{\dot{N}}{N} = -G_1 - 2G_2 \bar{n} - \frac{8}{\sqrt{3}} G_3 \bar{n}^2, \quad (4)$$

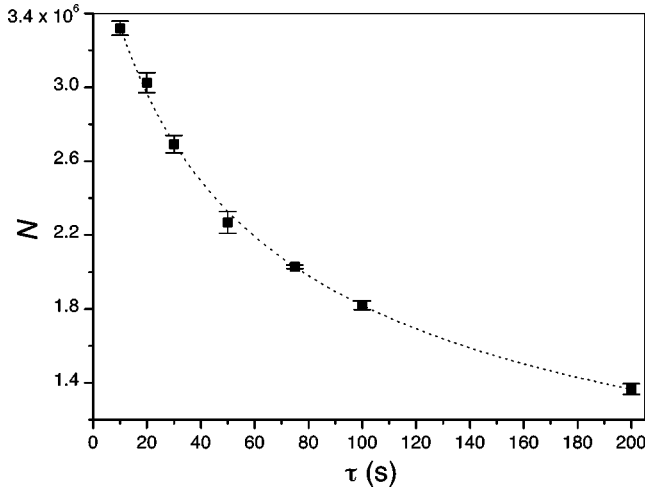


FIG. 1. Decay of the total number of trapped atoms  $N$  as a function of free evolution time  $\tau$  after the completion of evaporation. Each data point is the mean of several measurements and the error bars represent the standard deviation of the mean. The dotted line is a fit to the empirical function  $N(t) = N_0(1 + kt)^\gamma$ , giving  $N_0 = (3.88 \pm 0.09) \times 10^6$ ,  $k = (3.5 \pm 0.8) \times 10^{-2} \text{ s}^{-1}$ , and  $\gamma = -0.50 \pm 0.04$ .

where the average density  $\bar{n} = N[m\bar{\omega}^2/(4\pi k_B T)]^{3/2}$ . The rate constants  $G_i$  are obtained from Eq. (4) by determining  $N$  and  $\bar{n}$  at different times as the gas evolves freely.

The apparatus used in this experiment has been described previously [7]. The permanent magnet trap has a depth of 10 mK and a bias field of 1004 G at the trap center. Approximately  $5 \times 10^8$   $^7\text{Li}$  atoms are directly loaded into the trap from a laser slowed atomic beam using three-dimensional laser cooling. The loading saturates in about 1 s due to optical pumping into untrapped magnetic sublevels. Following loading, the laser beams are extinguished and the atoms are evaporatively cooled to the desired temperature by using a microwave field to selectively remove the hottest atoms. Evaporative cooling increases the atomic density and thus the collision rates which are being measured. Evaporation is stopped at  $\sim 2 \mu\text{K}$  with  $\sim 4 \times 10^6$  atoms, giving peak atomic densities of  $\sim 10^{12} \text{ cm}^{-3}$ . Under these conditions, the phase-space density is  $\sim 25$  times below that required for BEC. Following evaporation, the cold cloud is allowed to evolve freely. The microwave evaporation frequency is raised to 10 MHz above the spin-flip transition frequency at the trap center. This reduces the trap depth to 250  $\mu\text{K}$ , which ensures that all atoms undergoing dipolar relaxation collisions are lost. After a free evolution time  $\tau$ , the cloud is probed *in situ* using the phase-contrast imaging technique described in Ref. [7]. In this technique, an off-resonant probe laser beam is passed through the cloud and the scattered light is imaged onto a CCD camera. The resulting signal is proportional to the optical density of the cloud and is fit to a Gaussian function to find  $N$  and  $T$ , which together determine  $\bar{n}$ . In order to obtain low-noise and high-resolution images, destructive probing is used, so that only one image is obtained per evaporative cooling cycle. Therefore, the experiment is repeated many times and the results of several cycles are averaged at each value of  $\tau$ .

Figure 1 shows a plot of  $N$  versus  $\tau$ . The data points

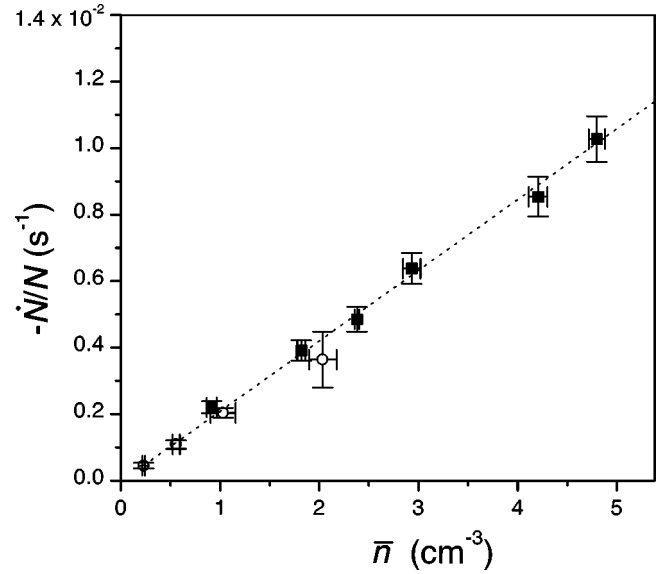


FIG. 2. The ratio  $\dot{N}/N = k\gamma/(1 + k\tau)$  as a function of the average atomic density  $\bar{n}$ . The black squares correspond to data shown in Fig. 1 and the open circles are from data taken on a different day. The vertical error bars are derived directly from the uncertainties in  $k$  and  $\gamma$  while the horizontal error bars represent the standard deviation in the mean of  $\bar{n}$  for several images taken at the same value of  $\tau$ . The dotted line is a fit to the function  $\dot{N}/N = -G_1 - 2G_2\bar{n} - (8/\sqrt{3})G_3\bar{n}^2$ , where  $G_1$  is the background gas collisional loss rate constant,  $G_2$  is the dipolar relaxation rate constant, and  $G_3$  is the three-body recombination rate constant.

represent the mean of several measurements and the error bars are the standard deviation of the mean. The dotted line is a fit to the data of the form  $N(t) = N_0(1 + kt)^\gamma$ , where  $N_0$ ,  $k$ , and  $\gamma$  are fit parameters. The purpose of this empirical function is to facilitate an accurate determination of  $\dot{N}$  from a small number of data points. The uncertainties in  $k$  and  $\gamma$  are the variations which increase the unreduced  $\chi^2$  by 1 [16]. We neglect data for  $\tau = 0$  s since these distributions have not equilibrated after evaporative cooling, and their inclusion introduces systematic errors in the determination of  $\bar{n}$ . After several elastic collision times, the gas should be well thermalized and these errors greatly reduced. For peak densities of  $\sim 10^{12} \text{ cm}^{-3}$  achieved in this experiment, the elastic collision rate is  $\sim 3$  Hz.

Along with the loss of atoms, a significant heating is observed in the trap. This heating is in part a result of dipolar relaxation as atoms are lost preferentially from the region near the trap center where the density is highest. Since the energy of atoms in this region is less than the average energy of the sample, the gas heats up. However, we find that a linear heating rate of 6 nK/s must also be included to account for the observed heating. As this additional heating is density independent, we surmise that it is due to either glancing collisions with background-gas atoms which impart insufficient energy to eject atoms from the trap or photon scattering from stray laser light. The effect of the heating is accounted for since the measured value of  $T$  is used in the calculation of  $\bar{n}$ .

The ratio  $\dot{N}/N = k\gamma/(1 + k\tau)$  is plotted as a function of  $\bar{n}$  in Fig. 2. The horizontal error bars are the standard deviation

in the mean of  $\bar{n}$  for the group of images taken at each value of  $\tau$  and the vertical error bars are derived directly from the uncertainties in  $k$  and  $\gamma$ . The dotted line is a fit of Eq. (4) to the data giving  $G_1 = (-0.3 \pm 1.0) \times 10^{-4} \text{ s}^{-1}$ ,  $G_2 = (1.05 \pm 0.10) \times 10^{-14} \text{ cm}^3/\text{s}$ , and  $G_3 = (0.5 \pm 8.1) \times 10^{-28} \text{ cm}^6/\text{s}$ . The quoted uncertainties are dominated by statistical fluctuations in  $N$  and  $\bar{n}$ . However, a small part ( $< 20\%$ ) of the uncertainty in  $G_2$  arises because of a systematic uncertainty in the polarizer angle used in the phase-contrast polarization imaging technique [7].

We can only set upper bounds for  $G_1$  and  $G_3$  due to their large relative uncertainties. The upper bound for the background gas collisional loss rate constant  $G_1 \leq 10^{-4} \text{ s}^{-1}$  is consistent with a background gas pressure of  $\leq 10^{-12}$  torr obtained by extrapolating the loss rate from measurements at higher pressures. The upper bound for the three-body recombination rate constant  $G_3 \leq 10^{-27} \text{ cm}^6/\text{s}$  is too large to provide a stringent test of theory but is consistent with calculations performed by Moerdijk *et al.*, who find a value of  $2.6 \times 10^{-28} \text{ cm}^6/\text{s}$  at zero magnetic field [17]. The precise value obtained for  $G_2$  does provide a significant test of theory.

Moerdijk *et al.* calculate that  $G_2 = (9.35 \pm 0.20) \times 10^{-15} \text{ cm}^3/\text{s}$  for a magnetic field strength of  $10^3 \text{ G}$  [18], in good agreement with the measurement.

The agreement between experimental measurements and theoretical calculations of the dipolar relaxation rate constant for both hydrogen and lithium indicates this process is well understood for light atoms, in contrast to cesium. It was suggested in Ref. [13] that a possible explanation for the disagreement in cesium arises because of the neglect of a second-order effect in the electronic spin-orbit coupling [19]. Evidently, this effect is negligible in atoms as light as lithium. In the future, we hope to measure similar quantities in  ${}^6\text{Li}$  and in a mixed-species gas of  ${}^6\text{Li}$  and  ${}^7\text{Li}$  because of the important role that inelastic collisions will play in the production of a quantum degenerate Fermi gas [20].

We are grateful to W. I. McAlexander for helpful discussions, and to B. J. Verhaar and his group for providing a numerical value for  $G_2$ . This work was supported by the National Science Foundation, the National Aeronautics and Space Administration, the U.S. Office of Naval Research, and the Welch Foundation.

- 
- [1] M. H. Anderson, J. R. Ensher, M. R. Matthews, C. E. Wieman, and E. A. Cornell, *Science* **269**, 198 (1995).
- [2] C. C. Bradley, C. A. Sackett, J. J. Tollett, and R. G. Hulet, *Phys. Rev. Lett.* **75**, 1687 (1995).
- [3] K. B. Davis, M.-O. Mewes, M. R. Andrews, N. J. van Druten, D. S. Durfee, D. M. Kurn, and W. Ketterle, *Phys. Rev. Lett.* **75**, 3969 (1995).
- [4] W. Ketterle and N. J. van Druten, in *Advances in Atomic, Molecular, and Optical Physics*, edited by B. Bederson and H. Walther (Academic Press, San Diego, 1996), No. 37, p. 181.
- [5] C. A. Sackett, C. C. Bradley, and R. G. Hulet, *Phys. Rev. A* **55**, 3797 (1997).
- [6] C. C. Bradley, C. A. Sackett, and R. G. Hulet, *Phys. Rev. Lett.* **78**, 985 (1997).
- [7] C. A. Sackett, C. C. Bradley, M. Welling, and R. G. Hulet, *Appl. Phys. B: Lasers Opt.* **65**, 433 (1997).
- [8] A. Lagendijk, I. F. Silvera, and B. J. Verhaar, *Phys. Rev. B* **33**, 626 (1986).
- [9] H. T. C. Stoof, J. M. V. A. Koelman, and B. J. Verhaar, *Phys. Rev. B* **38**, 4688 (1988).
- [10] D. A. Bell, H. F. Hess, G. P. Kochanski, S. Buchman, L. Pollack, Y. M. Xiao, D. Kleppner, and T. J. Greytak, *Phys. Rev. B* **34**, 7670 (1986).
- [11] R. van Roijen, J. J. Berkhout, S. Jaakkola, and J. T. M. Walraven, *Phys. Rev. Lett.* **61**, 931 (1988).
- [12] N. Masuhara, J. M. Doyle, J. C. Sandberg, D. Kleppner, T. J. Greytak, H. F. Hess, and G. P. Kochanski, *Phys. Rev. Lett.* **61**, 935 (1988).
- [13] J. Söding, D. Guéry-Odelin, P. Desbiolles, G. Ferrari, and J. Dalibard, *Phys. Rev. Lett.* **80**, 1869 (1998).
- [14] E. Tiesinga, A. J. Moerdijk, B. J. Verhaar, and H. T. C. Stoof, *Phys. Rev. A* **46**, R1167 (1992).
- [15] S. Kadlecik, L. W. Anderson, and T. G. Walker, *Phys. Rev. Lett.* **80**, 5512 (1998).
- [16] P. R. Bevington and D. K. Robinson, *Data Reduction and Error Analysis for the Physical Sciences*, 2nd ed. (McGraw-Hill, New York, 1992).
- [17] A. J. Moerdijk, H. M. J. M. Boesten, and B. J. Verhaar, *Phys. Rev. A* **53**, 916 (1996).
- [18] A. J. Moerdijk and B. J. Verhaar, *Phys. Rev. A* **53**, R19 (1996); B. J. Verhaar, F. van Ableen, and S. Kokkelmans (private communication).
- [19] P. S. Julienne and M. Krauss, *J. Mol. Spectrosc.* **56**, 270 (1975).
- [20] H. T. C. Stoof, M. Houbiers, C. A. Sackett, and R. G. Hulet, *Phys. Rev. Lett.* **76**, 10 (1996).